BIOCHEMISTRY
including biophysical chemistry & molecular biology
Current Topic

Biochemistry **2009,** *48,* 8083–8093 8083
DOI: 10.1021/bi900914g

Mechanisms of Antimicrobial, Cytolytic, and Cell-Penetrating Peptides: From Kinetics to Thermodynamics[†]

Paulo F. Almeida* and Antje Pokorny

Department of Chemistry and Biochemistry, University of North Carolina Wilmington, North Carolina 28403

Received June 1, 2009; Revised Manuscript Received July 7, 2009

ABSTRACT: The mechanisms of six different antimicrobial, cytolytic, and cell-penetrating peptides, including some of their variants, are discussed and compared. The specificity of these polypeptides varies; however, they all form amphipathic α-helices when bound to membranes, and there are no striking differences in their sequences. We have examined the thermodynamics and kinetics of their interaction with phospholipid vesicles, namely, binding and peptide-induced dye efflux. The thermodynamics of binding calculated using the Wimley−White interfacial hydrophobicity scale are in good agreement with the values derived from experiment. The generally accepted view that binding affinity determines functional specificity is also supported by experiments in model membranes. We now propose the hypothesis that it is the thermodynamics of the insertion of the peptide into the membrane, from a surface-bound state, that determine the mechanism.

During the past three decades, a vast number of antimicrobial peptides (*1*, *2*) and other related cytolytic peptides (*3*) have been discovered and their mechanisms examined. More recently, several cell-penetrating peptides have been described, which allow for transport of large molecules, such as proteins or DNA fragments, into cells (*4*−*8*). Perhaps surprisingly, many of these antimicrobial, cytolytic, and cell-penetrating peptides fall into the same structural class. They form an amphipathic α-helix of some 14−40 residues, when bound to a membrane surface, yet they show remarkable specificity regarding the target membrane or organism. What has befuddled researchers for a long time is the absence of a correlation between sequence and function or mechanism. The only element that appears to separate antimicrobial from cytolytic peptides is the fact that antimicrobials are usually cationic. This provides a simple explanation for their specificity because cationic peptides should bind better to the anionic membranes of most bacteria than to the neutral membranes of eukaryotic cells (*9*).

We now critically review results obtained over the past several years on a set of representative antimicrobial, cytolytic, and cell-penetrating peptides. The interactions of these peptides with model membranes were all studied with the same methods and under similar conditions. Experiments using small unilamellar vesicles (SUVs)[1] were common in the past, but we purposely exclude them because of the strained nature of those vesicles, concentrating instead on studies that use unstrained vesicles, such as large (LUVs) or giant unilamellar vesicles (GUVs). The results are, therefore, directly comparable. On the basis of a quantitative analysis of the kinetics and thermodynamics of these interactions, we propose the hypothesis that the peptide sequence specifies the mechanism only indirectly, through the thermodynamics of the insertion of the peptide into the bilayer medium from the surface-bound state. This would explain the lack of direct correlation between sequence and mechanism.

Beyond interactions with simple model lipid membranes, many questions remain regarding the function of antimicrobial and cytolytic peptides, which will not be discussed here. For example, the cell membrane is probably heterogeneous; it is likely to contain regions where peptides partition preferentially and regions from which they are excluded. We have suggested that this results in concentration of the peptides in preferred regions, increasing their efficacy (*10*, *11*). Also, the role of membrane proteins is virtually unexplored. It is well-known that there are no specific cell-surface receptors for these peptides (*12*, *13*), but their binding and insertion into the membrane may be influenced by other proteins. Another question is the functional role of peptide oligomerization in aqueous solution. δ-Lysin, for example, forms a four-helix bundle, with the hydrophobic residues inside, shielded from water (*14*). One possibility is that self-association is a strategy for avoiding hydrolysis by proteases, but this question is also unresolved.

A SET OF REPRESENTATIVE AMPHIPATHIC, α-HELICAL PEPTIDES

We have examined the binding to membranes and the mechanism of membrane perturbation or disruption of a small group of peptides, which represent different chemical properties and

[†]This work was supported by National Institutes of Health Grant GM072507.

*To whom correspondence should be addressed. Telephone: (910) 962-7300. Fax: (910) 962-3013. E-mail: almeidap@uncw.edu.

[1]Abbreviations: SUV, small unilamellar vesicle; LUV, large unilamellar vesicle; GUV, giant unilamellar vesicle; Tp10, transportan 10; POPC, 1-palmitoyl-2-oleoyl-*sn*-glycero-3-phosphocholine; POPG, 1-palmitoyl-2-oleoyl-*sn*-glycero-3-phosphoglycerol; DOPC, 1,2-dioleoyl-*sn*-glycero-3-phosphocholine; SOPC, 1-stearoyl-2-oleoyl-*sn*-glycero-3-phosphocholine; 7MC, 7-methoxycoumarin-3-carboxylic acid; ANTS, 8-aminonaphthalene-1,3,6-trisulfonic acid; DPX, *p*-xylene-bis-pyridinium bromide; FRET, fluorescence resonance energy transfer; NMR, nuclear magnetic resonance; CD, circular dichroism; P/L, peptide-to-lipid ratio; MPEx, Membrane Protein Explorer; ΔG°_{if}, Gibbs energy of peptide binding to the membrane−water interface as a helix; ΔG°_{oct}, Gibbs energy of transfer of the peptide from water to octanol; $\Delta G^\circ_{oct\text{-}if} = \Delta G^\circ_{oct} - \Delta G^\circ_{if}$; ΔG°_{ins}, Gibbs energy of insertion from the surface into the membrane; ΔG°_{bind}, Gibbs energy of binding derived from experiment; ΔG°_f, Gibbs energy of folding to an α-helix in water; T_m, helix−coil transition temperature; k_{on}, on-rate constant; k_{off}, off-rate constant; K_D, equilibrium dissociation constant.

Published on Web 08/05/2009

Table 1: Peptides Examined

peptide	charge (pH 7)	length (no. of amino acids)	sequence
δ-lysin	0	26	formyl-MAQDIISTIGDLVKWIIDTVNKFTKK
Tp10	+5	21	AGYLLGKINLKALAALAKKIL-amide
Tp10-COO^-	+4	21	AGYLLGKINLKALAALAKKIL
Tp10W	+5	21	AGWLLGKINLKALAALAKKIL-amide
Tp10W-COO^-	+4	21	AGWLLGKINLKALAALAKKIL
Tp10−7MC	+4	21	AGYLLGK(-7MC)INLKALAALAKKIL-amide
cecropin A	+7	37	KWKLFKKIEKVGQNIRDGIIKAGPAVAVVGQATQIAK-amide
magainin 2	+3	23	GIGKFLHSAKKFGKAFVGEIMNS
mastoparan	+4	14	INLKALAALAKKIL-amide
mastoparan X	+4	14	INWKGIAAMAKKLL-amide
melittin	+6	26	GIGAVLKVLTTGLPALISWIKRKRQQ-amide

biological specificities (Table 1). The peptides selected were the hemolytic peptide δ-lysin from *Staphylococcus aureus*, the antimicrobial peptides cecropin A from the moth *Hyalophora cecropia* and magainin 2 from the frog *Xenopus laevis*, the cytotoxic mastoparans from the wasps *Vespula lewisii* (mastoparan) and *Vespa xanthoptera* (mastoparan X), and the synthetic, cell-penetrating peptide transportan 10 (Tp10). To these we have added melittin, from bee (*Apis mellifera*) venom, which has been extensively studied by other authors and will also be discussed here. All these peptides form amphipathic α-helices, but they differ in length, charge, and specificity, thus spanning a broad range of properties.

Various models have been proposed for the function of these amphipathic peptides, such as the barrel-stave (*15*), toroidal-pore (*16*, *17*), sinking-raft (*18*−*20*), and carpet models (*21*, *22*). Huang and collaborators have proposed that membrane thinning, which is a consequence of peptide binding, is a critical determinant of membrane perturbation and pore formation (*23*). The peptides initially bind to the membrane surface and cause bilayer thinning until the peptide-to-lipid ratio (P/L) reaches a certain threshold, P/L*. Beyond this point, no more thinning occurs and peptides begin to insert into the membrane. This threshold in membrane thinning coincides closely with a change from an orientation parallel to the membrane surface to an inserted state, observed by oriented circular dichroism (*23*, *24*). The value of P/L* depends somewhat on the peptide and the lipid but is typically close to 1:50 (*23*, *24*). Above P/L*, the inserted state appears to form pores that are equilibrium structures, whereas for peptide concentrations below this threshold, only transient pores form (*24*). The conformation of the lipid bilayer around these pores has been recently investigated by X-ray diffraction (*25*). A Bax-derived peptide allows a continuous, curved bilayer around the pore, consistent with a toroidal pore, which has been proposed for magainin 2 and melittin (*26*). On the other hand, alamethicin leads to a complete interruption of the bilayer, consistent with a barrel-stave pore. It should be mentioned, however, that a recent study of alamethicin in membranes proposes a model that is very different from a static barrel-stave pore; rather, the function of alamethicin is explained by the formation of transient pores that result from random association of alamethicin peptides inserted perpendicular to the membrane (*27*).

The current consensus is that cytolytic and antimicrobial peptides kill their target cells by membrane disruption or perturbation, and even cell-penetrating peptides must transiently perturb the membrane as they gain access to the cell interior. Instead of focusing on the different types of molecular models, we have concentrated on trying to understand peptide-induced dye efflux kinetics. Kinetic rather than equilibrium data were used because the peptide mechanism can involve a transient pore, which may not correspond to the most populated peptide state. Moreover, the final, equilibrium state obtained via addition of peptides to lipid membranes may tell us little about the mechanism of membrane disruption or perturbation. As also recently remarked by Huang and collaborators, "pore formation in cell membranes caused by water-soluble peptides typically occurs as a kinetic process" (*24*).

What is the rate-limiting step in this process? We may subdivide it into three steps: pore formation, finding the pore by an entrapped particle, and crossing the pore. The characteristic time for crossing the pore itself is approximately $h^2/(2D)$, where h is the length of the pore and D is the diffusion coefficient. Crossing the pore is not rate-limiting. With an h of 50 Å (bilayer thickness), this time is on the order of 100 ns, which is in agreement with recent simulations for ions through protegrin pores (*28*, *29*). Even if a free energy barrier of ∼5 kcal/mol is assumed for crossing the pore, this time only increases to 1 ms. The characteristic time of escape of a small particle from a sphere of volume V through a small hole of radius a is on the order of $V/(2Da)$ (*30*, *31*). Thus, the time for efflux of the contents of an LUV, with a diameter of 0.1 μm, through a pore ∼20 Å in diameter is ∼1 ms. Escape times of ∼10 ms were obtained from simulations (*32*). For a GUV, with a diameter of 10 μm, a similar calculation yields 1000 s, but experimentally efflux from a single vesicle occurs in ∼10 s (*33*), indicating that many pores form or that they are much larger in GUVs. In conclusion, the efflux times from a single vesicle are much shorter than those observed experimentally in peptide-induced efflux from a vesicle population. This tells us two important things about the mechanism of antimicrobial peptides: a single pore is sufficient to cause rapid release of contents from a large vesicle (LUV), and if such a pore forms, the dye efflux times measured experimentally in a vesicle population reflect mainly the time of pore formation (*34*).

We have measured the kinetics of binding of a peptide to membranes and peptide-induced dye efflux from LUVs under similar conditions, namely, at P/L values of 1:50 to 1:100 or less, with peptide and lipid concentrations of 0.5−1 and 25−500 μM, respectively, for the chosen set of peptides, δ-lysin, Tp10, mastoparans, cecropin A, and magainin 2 (*18*−*20*, *35*−*38*). Kinetic models of possible mechanisms were tested using a global theoretical analysis (*18*, *19*), by directly fitting the sets of differential equations that represent the kinetic models to the experimental, time-dependent data. Our experiments were performed at low P/L values, under which conditions only transient pores exist according to Huang's analysis. Therefore, there is no contradiction with respect to the existence of equilibrium pores

proposed by Huang's laboratory (*24*), or aggregation in the membrane, as shown recently for melittin (*39*), which may occur at higher P/L values. However, we maintain that it is not necessary to reach the high-P/L regime for these peptides to function.

The mechanisms of δ-lysin, Tp10, mastoparans, cecropin A, and magainin 2 can be explained by different molecular models. However, knowing the mode of dye release, we were able to divide them into two groups via a quantitative analysis of the kinetics of peptide binding and dye efflux, according to the type of kinetic mechanism, all-or-none (*35*, *36*) or graded (*18*−*20*, *37*) (Figure 1). Melittin induces graded dye release (*40*), but we have not modeled its kinetics. In both types of mechanisms, the peptides initially bind to the vesicle surface and accumulate there, creating a mass imbalance across the lipid bilayer, which perturbs the membrane. Beyond that point, there are differences between the two mechanisms, which affect the kinetics. In an all-or-none mechanism (*35*) (Figure 1, top), partitioning of the peptides into the bilayer interior is very unfavorable, as discussed below. Pores form transiently, as a stochastic process, probably initiated by a peptide-induced defect in the membrane, as if it were under tension (*24*, *41*−*44*). The presence of peptides stabilizes the pore (*44*), which allows the contents of the vesicle to leak out, essentially all at once. This is probably not a well-organized channel, since no significant peptide oligomerization occurs (*35*, *36*), but rather a somewhat disordered or "chaotic" (*45*) toroidal pore, lined mostly by lipids, with some associated peptides, as suggested by recent molecular dynamics simulations (*46*−*48*). Previously, we argued that peptide translocation is probably limited in this mechanism (*35*, *36*). However, while not essential for the all-or-none mechanism, peptide translocation across the membrane is not incompatible with the kinetics, even quantitatively, and it could occur to a significant extent, at least for some peptides, as proposed for magainin 2 (*17*). The lifetime of the pore is long enough so that the entire contents of the vesicle are released. This creates a population of empty vesicles, which increases in time in a dye efflux experiment, and influences the observed kinetics as they compete with the full vesicles for peptide binding (*35*). Recent experiments with GUVs have clearly demonstrated the all-or-none nature of dye release induced by magainin 2 (*33*, *49*), in agreement with our results (*36*). Other GUV kinetic experiments have supported the idea that the mechanism of pore formation is stochastic and similar to tension-induced membrane disruption (*24*).

On the other hand, in a graded mechanism (*18*−*20*, *37*) (Figure 1, bottom), the probability of a peptide transiently inserting into the hydrophobic core is greater, and peptide translocation across the bilayer may occur concomitant with membrane perturbation. In the bilayer-inserted state, which constitutes the apparent pore, the peptide "catalyzes" efflux of the dye from the vesicle lumen. As peptide translocation is completed, the mass balance across the bilayer is restored and the rate of efflux becomes very slow or eventually stops (*18*, *19*, *50*). That is, efflux ceases when the peptide population equilibrates across the bilayer. In principle, this is a dynamic equilibrium, where insertion could occur from both sides, but in this mechanism, the rate of insertion is negligible in the absence of a mass imbalance and consequent bilayer stress. Therefore, a significant amount of dye may remain inside each vesicle at the end of a dye efflux experiment, if peptide translocation is fast compared with the rate of dye efflux. In this kinetic model, all vesicles are equivalent; they can, in fact, be modeled as one enormous vesicle. No empty vesicles ever exist, except at the very end, if complete release is achieved. A model very similar to the one we proposed (*18*−*20*) was suggested from molecular dynamics simulations (*48*). It has been shown that graded and all-or-none release can be obtained as two extreme cases of a model in which the efflux time is either very long or very short compared to the pore lifetime (*51*). A "gray zone" may exist for intermediate situations, yet the differences between the two mechanisms noted above are important in modeling the release kinetics and may stem from significant differences in peptide structure, as discussed below.

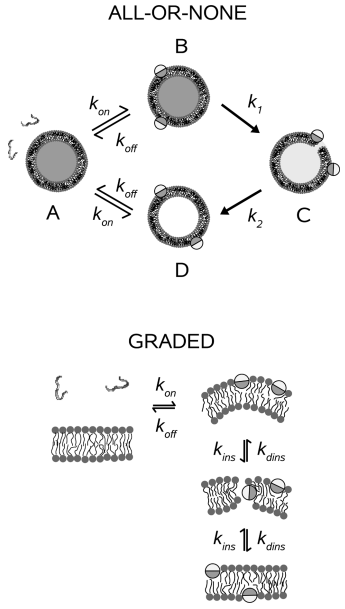

FIGURE 1: Models proposed for the mechanisms of peptides that cause all-or-none release (top) and graded release (bottom). The peptides are mostly unstructured in aqueous solution, but as they bind to the membrane, they and form an amphipathic α-helix, which is shown in cross section as a cylinder, the darker half-circles representing the hydrophobic face and the lighter half-circles the hydrophilic face. All-or-none mechanism (top) (*35*): (A) peptide in solution, (B) peptide bound to the membrane surface of dye-loaded vesicles, (C) peptide associated with vesicles in the pore state, which causes all-or-none efflux, and (D) peptide bound to an empty vesicle, from which it dissociates back into solution. In the graded mechanism (bottom) (*19*, *20*), binding of peptides creates a mass imbalance across the lipid bilayer, which perturbs the membrane, enhancing the probability of a peptide transiently inserting into the hydrophobic core and crossing the bilayer. In the bilayer-inserted state, the peptide causes efflux of the dye from the vesicle. As peptide translocation proceeds, the mass imbalance across the bilayer is dissipated and efflux decelerates, eventually stopping. Reproduced, with modifications, from refs *20*, *35*, and *36*. Copyright 2007, 2008, and 2009, respectively, Elsevier.

The two modes of dye release, graded and all-or-none, can be distinguished by a requenching experiment (*32*, *52*, *53*) in which a fluorophore, 8-aminonaphthalene-1,3,6-trisulfonic acid (ANTS), and a quencher, *p*-xylene-bis-pyridinium bromide (DPX), are both incorporated in the vesicle lumen. As peptides interact with the membrane, both the fluorophore and the quencher leak out at comparable rates. In graded release, the fluorescence of ANTS inside the vesicles increases because the quencher concentration decreases. Thus, a plot of the fluorescence inside against the fraction of ANTS released yields a rising curve (Figure 2, top), but in all-or-none release, the degree of quenching inside the vesicles is independent of the amount of ANTS and DPX released because only the intact vesicles contribute to the signal from inside the

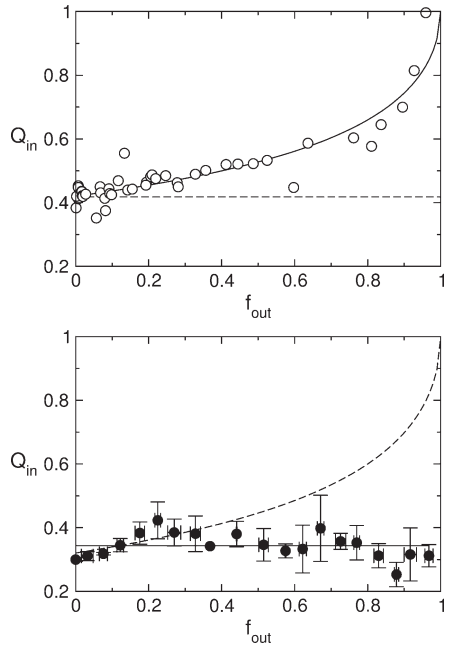

FIGURE 2: Fluorescence requenching (ANTS/DPX) assay for cecropin A in POPC/POPG LUVs (bottom) (*35*) and Tp10 in POPC/POPS LUVs (top) (*20*). The fluorescence quenching factor inside the vesicles, Q_{in}, is plotted against the fraction of fluorophore (ANTS) released, f_{out}. All-or-none release yields a horizontal line, indicating that the fluorescence inside the intact vesicles is independent of the amount of fluorophore released. Graded release yields a rising curve, because of relief of fluorescence quenching as DPX also leaks out of the vesicles. Reproduced, with modifications, from refs *20* and *35*. Copyright 2007 and 2008, respectively, Elsevier.

vesicles and the plot yields a horizontal line (Figure 2, bottom). Cecropin A and magainin 2 cause all-or-none release, and their kinetics are quantitatively described by an all-or-none kinetic mechanism (*35*, *36*). δ-Lysin, Tp10, and mastoparans cause graded release of vesicle contents, and their kinetics of dye efflux are described by a graded kinetic mechanism (*19*, *20*, *37*, *54*, *55*). They appear to translocate across the bilayer, Tp10 and mastoparans as monomers and δ-lysin as a small oligomer. Melittin also causes graded release (*40*) and appears to translocate across the bilayer (*56*). Cecropin A and magainin 2 appear to disrupt or perturb the vesicles through a chaotic pore event, which leads to leakage of the vesicle contents, essentially all at once. Most of the differences in efficiency of cecropin A and magainin 2 toward vesicles containing varying amounts of anionic lipids appear to be due to differences in binding (*35*, *36*). This conclusion was recently supported by experiments with GUVs, which showed that the ratio of bound peptide to lipid determined dye release kinetics induced by magainin 2 (*49*). According to our data, peptide oligomerization in membranes is not essential for dye release (*20*, *35*−*37*), except for δ-lysin, in which case it involves dimers, trimers, or at most tetramers (*18*, *19*).

THERMODYNAMICS OF PEPTIDE BINDING TO THE MEMBRANE

To understand the reasons for the two different types of behaviors, we have examined the thermodynamics of binding of the peptides to the surface of a 1-palmitoyl-2-oleoylphosphatidylcholine (POPC) membrane and their transfer to the bilayer hydrophobic interior (*20*, *38*) (Figure 3). The thermodynamics of association of a peptide with membranes were

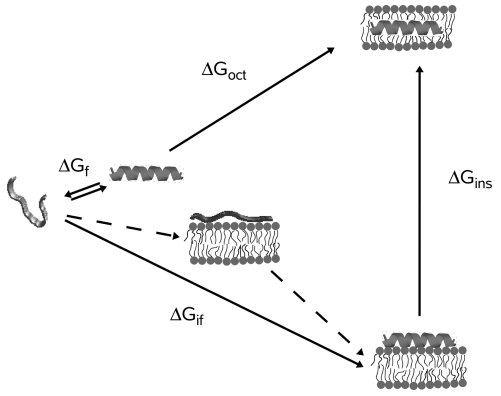

FIGURE 3: Thermodynamic cycle for peptide binding to the membrane interface and inserting into the bilayer core. In water, the equilibrium between unfolded and folded conformations, governed by ΔG_f, is usually shifted to the unfolded state. Binding to the membrane interface is governed by ΔG_{if} (bottom solid arrows). This is composed of two terms (dashed arrows), binding as an unfolded peptide and folding to a helix on the surface. Insertion into the bilayer core (ΔG_{ins}) can be approximated by $\Delta G_{oct\text{-}if}$ if ΔG_f is small. Reproduced, with modifications, from ref *20*. Copyright 2007 Elsevier.

obtained by measuring the kinetics of binding to LUVs of POPC or mixtures of POPC with anionic phospholipids (*20*, *35*−*38*). The kinetics were measured by stopped-flow fluorescence using the change in Förster resonance energy transfer (FRET) from a Trp residue on the peptide to a phospholipid labeled with the fluorophore 7-methoxycoumarin (7MC), which is incorporated in the bilayer (*35*−*38*). Occasionally, the changes in the fluorescence intensity of the Trp or a 7MC-modified lysine on the peptide were used instead of FRET (*20*). The measurements yield the on- and off-rate constants, k_{on} and k_{off}, from which the equilibrium dissociation constant is obtained as $K_D = k_{off}/k_{on}$.[2] The case of δ-lysin is complicated by its oligomerization in aqueous solution (*14*). At a concentration of 0.5 μM, which was used in the binding measurements (*57*), the peptide exists as a mixture of approximately 60% monomers and 40% dimers. This distribution is calculated from the tetramer and dimer dissociation constants that we previously estimated (*19*). The dimer is likely to bind more weakly than the monomer because the hydrophobic face of the amphipathic helix involved in dimerization in water is the same that binds to the membrane interface. Therefore, the experimental value of K_D (60 μM) (*57*) is likely to be close to the monomer dissociation constant.

To include the correct mixing entropy term, K_D needs to be converted to mole fraction units (*58*). This so-called "cratic correction" is applied by subtracting RT ln 55 from the Gibbs energy derived from K_D; that is, $\Delta G^\circ_{bind} = RT \ln K_D - 2.4$ kcal/mol at room temperature. We should note that the cratic

[2]As long as k_{on} refers to binding to vesicles, the meaning of K_D is clear. If one tries to relate it to lipid concentrations, the question arises regarding dividing K_D by 2 to correct for binding to the outer monolayer only. Whether this is appropriate depends on whether the peptides translocate across the membrane. If they do, the lipid chemical potential is determined by the entire bilayer and division by 2 is not appropriate. We have observed small differences in k_{off} values obtained from association and dissociation kinetics, by a factor of ~2 on average (*35*, *36*, *38*), slower if measured from dissociation reactions. This suggests that translocation occurs to some extent, concomitant with membrane perturbation or pore formation by the peptide. Therefore, we prefer to leave K_D undivided. If the experimental measurements reflected binding only to the outer monolayer of the vesicles, the term $-RT \ln 2 = -0.4$ kcal/mol would have to be added to the Gibbs energy of binding (ΔG°_{bind}) obtained from K_D. This level of uncertainty is present in all these calculations.

Table 2: Thermodynamic Parameters for Peptide Binding and Insertion into POPC Bilayers at Room Temperature

peptide	K_D[a]	ΔG°_{bind}(exp)[b] (kcal/mol)	ΔG°_{if}(calcd) (kcal/mol)	% helix	ΔG°_{oct} (kcal/mol)	$\Delta G^\circ_{oct\text{-}if}$ (kcal/mol)
δ-lysin	60 μM	−8.1	−4.7	90	21.9	26.6
δ-lysin with two salt bridges			−8.7		13.9	22.6
Tp10W	140 μM	−7.6	−7.8	60	9.3	17.1
Tp10W-COO^-	200 μM	−7.4	−5.9		13.6	19.5
Tp10−7MC[d]	20 μM	−8.7	−8.8		7.2	16.0
Tp10			−6.9		10.7	17.6
Tp10-COO^-			−5.0		15.0	20.0
cecropin A	1 mM	−6.4	−2.7	70	31.1	33.8
cecropin A with two salt bridges			−6.7		23.1	29.8
magainin 2 (F12W)[e]	5 mM	−5.5	−6.0	83	20.3	26.3
mastoparan X	300 μM	−7.2	−6.9	86	8.7	15.6
mastoparan			−4.9	70	8.3	13.2
melittin	100 μM	−7.8[f]	−7.4	70	12.0	19.4

[a] K_D is expressed in terms of lipid concentration, not vesicle concentration. To refer it to vesicle concentrations, the values reported must be divided by 10^5, since there are approximately 10^5 lipids in one large unilamellar vesicle. [b] $\Delta G^\circ_{bind} = RT \ln K_D - 2.4$ kcal/mol. [c] The calculation performed with MPEx (*65*) for an acetylated N-terminus yields −5.8 kcal/mol for transfer to the interface and 20.0 kcal/mol to octanol. For a formylated N-terminus, we add 1.1 kcal/mol to account for the methyl group transfer to the interface (*63*) or 1.9 kcal/mol to account for the methyl group transfer to octanol (*89*). [d] The ΔG° calculated for Tp10−7MC are only rough estimates based on replacement of Lys7 with Tyr to mimic the aromatic coumarin (*38*). With this replacement, the calculated ΔG°_{if} of −8.8 kcal/mol matches the experimental ΔG°_{bind} value of −8.7 kcal/mol. Replacement by Trp would yield a ΔG°_{if} of −9.7 kcal/mol. The purpose is to obtain a match with the binding experiment that can be used for the calculation of transfer to octanol, which is not experimentally accessible. [e] Binding was assessed with the F12W mutant. Calculations with a neutral His7 yield values of −6.1 and 20.1 kcal/mol for partitioning to the interface and to octanol, respectively; with a positively charged His7, values of −5.4 and 22.3 kcal/mol, respectively, are obtained. The weighted averages at pH 7.5 yield the values listed. [f] This value is the average of five measurements from different laboratories (7.8 ± 0.6 kcal/mol), including determinations in POPC (*85*, *87*), 1-stearoyl-2-oleoylphosphatidylcholine (SOPC), and DOPC (*86*) and values obtained from measurements in POPC/POPG mixtures by subtraction of the electrostatic component (*39*). The value of K_D listed is derived from the same average.

correction is a controversial issue (*59*−*61*), but for the sake of consistency with the work of White and Wimley (*58*), we follow their recommendation and apply this correction to our values. The Gibbs energy of binding to the membrane−water interface, ΔG°_{if}, can be calculated with the Wimley−White interfacial scale (*62*), which was extended to include transfer of several different types of amino- and carboxy-terminal groups to the membrane interface (*63*). The binding process is a coupled binding−folding event (*58*) whereby a peptide, mostly disordered in aqueous solution, binds and folds to an α-helix on the membrane surface (Figure 3, dashed arrows). When an amphipathic helix forms at the interface, the Gibbs free energy of the peptide is reduced by ∼0.4 kcal/mol per residue (*64*). Thus, ΔG°_{if} is the sum of two terms, representing binding in an unfolded state and folding at the interface. The results of the calculations for this set of peptides, performed with Membrane Protein Explorer [MPEx (*65*)], are listed in Table 2. To calculate ΔG°_{if}, the degree of helicity of the peptides needs to be obtained from experiment or estimated reliably. δ-Lysin is 73% helical on a micelle surface (*66*, *67*), but our circular dichroism (CD) measurements indicate ∼90% helical content on POPC vesicles (L. Huskins and P. F. Almeida, unpublished observations). Mastoparan X is ∼86% helical on a membrane surface (*68*), and mastoparan is ∼70% helical, taking into account several estimates (*69*−*71*). There are no helicity measurements on Tp10 or most of its variants, but we have estimated by CD that Tp10W is ∼60% helical on 1:1 POPC/1-palmitoyl-2-oleoyl-*sn*-glycero-3-phosphoglycerol (POPG) membranes (L. Huskins and P. F. Almeida, unpublished observations). This falls within the values of 53% for transportan (*72*), the parent peptide from which Tp10 is derived by a deletion of the six N-terminal residues, and 70% for mastoparan, whose sequence constitutes the 14 C-terminal residues of Tp10, of a total of 21 residues. Magainin 2 is ∼83% helical on a membrane based on NMR data (*73*), which we think is the most reliable estimate; other reported estimates range from ∼55 to >90% (*74*−*80*). Cecropin A is ∼80% helical in a hexafluoroisopropnanol/water solution (*81*, *82*) and essentially maintains the same helical structure when bound to membranes (*83*); our CD measurements yield ∼70% helical content (L. Huskins and P. F. Almeida, unpublished observations). Melittin is ∼70% helical on POPC or POPG membranes (*64*); other reported values range from ∼65 to 85% on POPC/POPG mixtures (*39*, *84*).

The agreement between the experimental (ΔG°_{bind}) and calculated (ΔG°_{if}) Gibbs energies of binding is very good for Tp10W, mastoparan X, magainin 2, and melittin (Table 2). For Tp10W, $\Delta G^\circ_{bind} = -7.6$ kcal/mol (*38*) and $\Delta G^\circ_{if} = -7.8$ kcal/mol. For mastoparan X, $\Delta G^\circ_{bind} = -7.2$ kcal/mol (*37*) and $\Delta G^\circ_{if} = -6.9$ kcal/mol. For magainin 2 (F12W variant), $\Delta G^\circ_{bind} = -5.5$ kcal/mol (*36*) and $\Delta G^\circ_{if} = -6.0$ kcal/mol. For melittin, $\Delta G^\circ_{bind} = -7.8$ kcal/mol (*39*, *85*−*87*) and $\Delta G^\circ_{if} = -7.4$ kcal/mol.

However, for δ-lysin and cecropin A, the calculated ΔG°_{if} values are in poor agreement with the experimental values. For cecropin A, $\Delta G^\circ_{if} = -2.7$ kcal/mol whereas $\Delta G^\circ_{bind} = -6.4$ kcal/mol (*35*), and for δ-lysin, $\Delta G^\circ_{if} = -4.7$ kcal/mol whereas $\Delta G^\circ_{bind} = -8.1$ kcal/mol (*57*). What is the reason for this discrepancy? We think that the disagreement is due to formation of salt bridges (hydrogen-bonded ion pairs) between positively and negatively charged functional groups of the peptide. None of the peptides whose calculated ΔG°_{if} agrees with ΔG°_{bind} obtained from experiment (magainin 2, melittin, mastoparan X, and Tp10 variants) can possibly establish intramolecular salt bridges. On the other hand, judging by their sequences, cecropin A could establish a maximum of two and δ-lysin probably three intramolecular salt bridges, in a helical structure (Table 1). Cecropin A may contain an $(i + 3)$K,E salt bridge between Lys6 and Glu9 and an $(i + 4)$D,K salt bridge between Asp17 and Lys21. According to Marqusee and Baldwin (*88*), $(i + 4)$ salt bridges stabilize the α-helix more than $(i + 3)$ salt bridges, and E,K salt bridges stabilize the α-helix more than K,E salt bridges. Therefore, we expect the $(i + 4)$D,K salt bridge to be especially strong.

δ-Lysin could make an ($i + 3$)D,K salt bridge between Asp11 and Lys14 and an ($i + 4$)D,K salt bridge between Asp18 and Lys22. In addition, it is possible that a salt bridge is established between one of the terminal lysines and the free terminal carboxylate. Alternative patterns involving an ($i + 4$)K,D salt bridge between Lys14 and Asp18 are also possible. In octanol, formation of an intramolecular salt bridge between acidic and basic groups of the peptide has been estimated to lower its Gibbs free energy by 4 kcal/mol (*89*). On the POPC membrane interface, this contribution must be smaller but still favorable (*62*). The free energies of transfer of charged residues from water to the interface are smaller than those of transfer to octanol by a factor of roughly 2 (*58*). We conjecture that, similarly, the free energy of salt bridge formation at the POPC−water interface will be smaller than in octanol by approximately the same factor, corresponding therefore to ~2 kcal/mol. This value appears to be reasonable because formation of a salt bridge in water, on the surface of a globular protein, contributes ~1 kcal/mol to protein stability. Hence, if δ-lysin were to form two salt bridges when bound to the membrane surface, ΔG°_{if} would equal −8.7 kcal/mol, in good agreement with the value obtained from experiment ($\Delta G^\circ_{bind} = -8.1$ kcal/mol), and if cecropin A were to form two salt bridges, ΔG°_{if} would equal −6.7 kcal/mol, which compares to the ΔG°_{bind} of −6.4 kcal/mol derived from experiment (Table 2).

Overall, the Wimley−White procedure provides very reasonable estimates of Gibbs energies of binding to POPC membranes. For peptides possessing cationic and anionic groups within hydrogen bonding distance, experimental and calculated binding Gibbs energies can be reconciled if formation of salt bridges is taken into account. For the sake of completeness, let us note that a different approach to determining peptide binding thermodynamics has been developed by Seelig's group (*39*, *84*, *85*, *90*, *91*) and that there are a few discrepancies in some of the free energies obtained. For instance, according to Ladokhin and White (*64*), the Gibbs energy is reduced by ~0.4 kcal/mol per residue upon folding to a helix at the interface, but the estimate from Seelig's group is a factor of 2 smaller, ~0.2 kcal/mol per residue (*39*, *90*, *91*). This is somewhat compensated by a more favorable free energy of binding of the unfolded state than calculated using the Wimley−White interfacial hydrophobicity scale. A discussion of the possible origins of these differences is beyond the scope of this work, but a few comments are justified. Since the binding of cationic polypeptides to zwitterionic membranes of pure POPC or dioleoylphosphatidylcholine (DOPC) is typically weak, because of the unfavorable Gibbs energy of partitioning of the peptide cationic side chains to the bilayer−water interface, Seelig and collaborators have assessed binding to POPC/POPG mixed vesicles, containing variable amounts of the anionic lipid, and have then factored out the electrostatic effects to obtain a "bare" partition constant. Those electrostatic effects, which include attraction between the peptide and the anionic lipid and repulsion between peptides, are estimated using Gouy−Chapman theory by a combination of calculation and fitting to experimental data (*39*, *84*, *85*). What is less clear is whether and to what extent the interactions between positive charges on the peptide and the zwitterionic bilayer interface are lumped into the electrostatic component of the binding constant, not explicitly, but implicitly, through the fitting procedure. This could lead to a reduction of their unfavorable effect on partitioning, leading to an overestimate of the bare binding constants. While both the Wimley−White and Seelig approaches provide reasonable estimates of Gibbs binding energies for binding to the bilayer interface, mixing elements of the two is likely to yield incorrect results because compensation of small inaccuracies, which probably exist within each method, would be lost. At this point, only the Wimley−White procedure can be used to calculate Gibbs binding energies for an arbitrary peptide and they agree well with the values derived from experiment, but we should keep in mind that there are alternative approaches and unresolved issues.

THERMODYNAMICS OF INSERTION OF A PEPTIDE INTO THE BILAYER

Let us now examine the thermodynamics of peptide transfer, as an α-helix, from a POPC membrane interface to the bilayer hydrophobic interior, using again the approach of White and Wimley (*58*). The relevant Gibbs energies of transfer for the set of peptides examined are listed in Table 2. The concept is illustrated in Figure 3 (*20*). A peptide is transferred from water to the membrane surface and from the surface to the bilayer interior. To complete the thermodynamic cycle, the Gibbs energy of folding (ΔG°_f) of a peptide to an α-helix in aqueous solution must be included. This value is generally not known for most peptides, but it is probably small. The number of degrees of freedom "frozen" in a coil−helix transition is ~10 per residue. This number can be understood in a simplified but intuitive manner if we consider that, in a random coil, there are three well-defined minima for the values of the ϕ and ψ dihedral angles (*92*). Therefore, each residue has approximately nine discrete conformations in a random coil, which are reduced to one in an α-helix. This is, of course, only a very rough approximation because the three minima are not equivalent and they are not discrete states. Nevertheless, several estimates of the entropy change associated with the coil−helix transition yield values that correspond to freezing ~10 degrees of freedom ($\Delta S \approx -R \ln 10 \approx -4.5$ cal K^{-1} mol^{-1} per residue). Schellman (*93*, *94*) estimated the reduction in entropy upon folding into a helix to be between 4 and 5 cal K^{-1} mol^{-1}. Brandts (*95*) arrived at a similar value (5.1 cal K^{-1} mol^{-1}), and Privalov (*96*), on the basis of the entropy of unfolding for a set of proteins, estimated the conformational entropy change per residue to be 4.2 cal K^{-1} mol^{-1}. The Gibbs free energy change for the coil−helix transition in water (ΔG°_f) can be calculated using an all-or-none model with end effects or the zipper model (*94*, *97*). More sophisticated approaches, such as the Zimm−Bragg (*98*) or Lifson−Roig (*99*) theories, are not justified for this simple estimate. Alanine-based peptides of 14−38 residues have helix−coil transition temperatures (T_m) in aqueous buffer varying from −10 to 35 °C (*100*). Using the values of T_m for this set of peptides and a value of 4.5 cal K^{-1} mol^{-1} for the conformational entropy change, the all-or-none or zipper models for the coil−helix transition yield a ΔG°_f of approximately ±2 kcal/mol, unfavorable for the smaller peptides and favorable for the longer ones in this set. These peptides were originally designed to establish salt bridges (*88*), so they might be expected to form more stable helices; however, another set of alanine-based peptides that cannot make salt bridges also forms stable helices in aqueous solution (*101*). In water, most antimicrobial peptides are primarily unstructured, but the order-of-magnitude estimate of ΔG°_f is probably valid.

The Gibbs energy of transfer of peptides from water to octanol can be obtained from the whole-residue octanol transfer scale (*102*). Although the bilayer interior is not similar to octanol, it turns out that the transfer of an α-helical polypeptide from water to the bilayer hydrophobic interior can be reasonably

estimated from the free energies of transfer from water to octanol, ΔG°_{oct} (*103*). The Gibbs energy for insertion into the bilayer nonpolar interior (ΔG°_{ins}) of a helical peptide bound to the membrane interface is obtained by closing the thermodynamic cycle [$\Delta G^\circ_{ins} = \Delta G^\circ_f + \Delta G^\circ_{oct} - \Delta G^\circ_{if}$ (Figure 3)]. To a fairly good approximation, $\Delta G^\circ_{ins} \approx \Delta G^\circ_{oct} - \Delta G^\circ_{if} = \Delta G^\circ_{oct\text{-}if}$, because ΔG°_f for folding in water is much smaller than all the other terms. Inspection of Table 2 reveals an interesting fact. $\Delta G^\circ_{oct\text{-}if}$ is ~20 kcal/mol or less for peptides that cause graded dye release, which includes mastoparans, Tp10, melittin, and δ-lysin, with $\Delta G^\circ_{oct\text{-}if} \approx$ 15, 17, 19, and 22 kcal/mol; however, $\Delta G^\circ_{oct\text{-}if} >$ 25 kcal/mol for peptides that cause all-or-none release, which includes magainin 2 and cecropin A, with $\Delta G^\circ_{oct\text{-}if} \approx$ 26 and 30 kcal/mol. All uncertainties in experimental and calculated values of Gibbs energies of transfer notwithstanding, this suggests that insertion is easier for peptides that follow a graded mechanism.

At this point, we want to make clear that we do not mean that antimicrobial and cytolytic peptides work by partitioning into the bilayer hydrophobic core. What we suggest is that the Gibbs energy of transfer from the interface to the bilayer hydrophobic core, estimated by $\Delta G^\circ_{oct\text{-}if}$, provides a tool for predicting the behavior of the peptides. The idea is that the thermodynamics of pore formation reflect the thermodynamics of insertion, however perturbed the bilayer may be by interaction with the peptide, in an extreme case with formation of a pore.

Finally, we consider briefly a different class, that of polycationic cell-penetrating peptides, which includes penetratin (*4*), the HIV-1 TAT peptide (*5*, *6*), polyarginine, and polylysine, for example. These peptides have been shown to cross membranes and even layers of nonpolar solvents, provided that phosphate-containing or other anionic counterions are present (*104*−*108*). They do not form α-helices and bind very weakly to zwitterionic membranes, and their mechanism may be unrelated to that of the amphipathic, α-helical peptides discussed here, which include the cell-penetrating peptide Tp10 and its variants. Yet, it is curious that application of the Wimley−White hydrophobicity scales to many of those polycationic peptides yields $\Delta G^\circ_{oct\text{-}if}$ values of < 20 kcal/mol. For example, for the TAT peptide (YGRKKRRQRRR), both transfer to the interface (ΔG°_{if} = 6.2 kcal/mol) and transfer to octanol (ΔG°_{oct} = 25.6 kcal/mol) are very unfavorable, but $\Delta G^\circ_{oct\text{-}if}$ = 19.4 kcal/mol. Similarly, for nonaarginine (acetyl-Arg_9-amide), ΔG°_{if} = 4.7 kcal/mol and ΔG°_{oct} = 18.3 kcal/mol, but $\Delta G^\circ_{oct\text{-}if}$ = 13.6 kcal/mol.[3] For nonalysine (acetyl-Lys_9-amide), ΔG°_{if} = 6.4 kcal/mol and ΔG°_{oct} = 27.2 kcal/mol, yielding a larger value ($\Delta G^\circ_{oct\text{-}if}$ = 20.8 kcal/mol). Experimentally, it is found that nonaarginine is more efficient than nonalysine (*109*) or TAT (*110*). At reasonable concentrations, these peptides will not bind to zwitterionic vesicles because of the very unfavorable, positive ΔG°_{if}. However, if the anionic lipid content of the membrane is sufficiently large, binding will occur. If the inserted or pore state is stabilized by a free energy similar to that of the surface-bound state in anionic vesicles relative to zwitterionic vesicles, which appears to be true for mastoparan X, Tp10, cecropin A, and magainin 2 (see next section), a situation can be achieved where these peptides bind but $\Delta G^\circ_{oct\text{-}if}$ is still below the threshold for translocation. Interesting suggestions regarding their mechanism come from molecular dynamics simulations (*48*). While the mechanisms of amphipathic (*46*, *47*) and polycationic cell-penetrating peptides (*48*) appear similar at first sight, in both cases involving formation of a disordered toroidal pore that includes one peptide or a few peptides, some subtle differences may be important. Particularly intriguing is the idea that arginine side chains of the cell-penetrating peptide reach out to the phosphate groups of the apposing leaflet of the bilayer, thus establishing hydrogen bonds and initiating the formation of a small pore (*48*).

[3]Usually, terminally modified versions of polycationic peptides have been used in the experiments, typically with a fluorescein chromophore on the N-terminus; therefore, we used N-terminal acetylated and C-terminal amidated sequences in the calculations, but free-terminal sequences would lead to the same qualitative conclusions.

RELATION TO DYE EFFLUX KINETICS

Consider a lipid vesicle to which a peptide binds from solution, eventually causing efflux of the vesicle contents. The graph of the Gibbs free energy profile for a hypothetical path that leads to insertion is shown in Figure 4. In the simplest scenario, the rate-limiting step for efflux should be the insertion of the peptide into the bilayer and its consequent perturbation. That rate is dominated by the exponential factor $e^{-\Delta G^\ddagger/RT}$, where $\Delta G^\ddagger$ is the activation energy barrier for peptide insertion. This process is unfavorable because of interactions between the peptide polar groups and the lipid acyl chains, and therefore, the inserted peptide is a high-free energy state. According to Hammond's postulate (*111*), we can assume that it lies close to the transition state (‡) and should resemble it. Therefore, the Gibbs energy of transfer from the membrane interface to the bilayer interior (ΔG°_{ins}) should be approximately equal to the Gibbs activation energy for insertion into the bilayer hydrophobic core ($\Delta G^\ddagger$). If ΔG°_f is small, as presumed, this argument provides an easy way to estimate $\Delta G^\ddagger \approx \Delta G^\circ_{oct\text{-}if}$, which can be calculated using the Wimley−White transfer scales. Membrane reorganization, including pore formation, will lower the actual activation energy considerably.

For cationic peptides, efflux from vesicles containing anionic lipids is much faster than from POPC vesicles. It turns out that for Tp10, cecropin A, magainin 2, and mastoparan X the rates of pore formation obtained from our fits do not depend very much on anionic lipid content. However, increasing anionic lipid content clearly enhances binding (*35*, *36*). This suggests that, as the Gibbs energy of the interface-bound state (G°_{if}) decreases with an increasing anionic lipid content, the Gibbs energy of the transition state ($G^\ddagger$) also decreases by a similar amount (Figure 4). In fact, the rates of pore formation obtained for cecropin A and magainin 2 depend little on anionic lipid content (*35*, *36*), which is consistent with $\Delta G^\ddagger$ remaining approximately constant. We have also observed this parallel change of calculated $\Delta G^\ddagger$ and ΔG_{bind} for Tp10 variants in mixtures of POPC with anionic lipids, leading us to suggest that, in anionic membranes, part of the binding energy is used to disturb the bilayer (*38*).

A WORKING HYPOTHESIS FOR THE MECHANISM OF ANTIMICROBIAL PEPTIDES

On the basis of the set of peptides examined, which is, admittedly, very limited, we propose the hypothesis that the mechanism of antimicrobial, cytolytic, and cell-penetrating peptides is determined by the thermodynamics of insertion into the membrane from the surface-bound state. Whether insertion actually occurs is another question. The interactions with the membrane are of course determined by the peptide sequence, but it is not the sequence directly that determines mechanism and

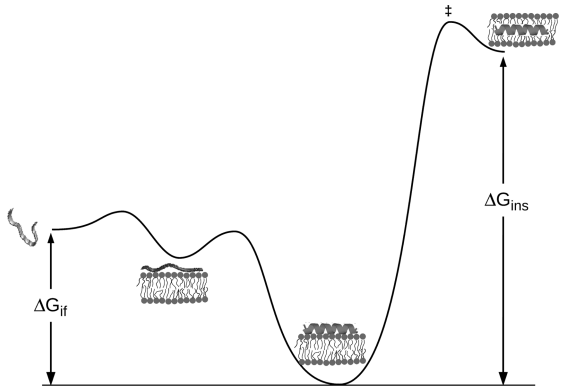

FIGURE 4: Reaction free energy diagram for the interaction of an amphipathic α-helical peptide with a phospholipid membrane. The meaning of the states is the same as in Figure 3.

specificity. This would explain why functionally determinant sequence motifs have not been found in antimicrobial peptides in spite of almost three decades of research.

We conclude with two predictions and two remarks.

1 If the Gibbs energy of insertion into the bilayer core is not too large ($\Delta G_{ins} \approx \Delta G^{\circ}_{oct\text{-}if} \leq 20$ kcal/mol), the peptides are predicted to follow a graded mechanism. They should translocate across the membrane, dissipating the bilayer mass imbalance that was generated by peptide binding, and cause graded efflux in the process. δ-Lysin, Tp10, mastoparans, and melittin appear to belong to this category. On the other hand, if $\Delta G_{ins} \approx \Delta G^{\circ}_{oct\text{-}if} \gg 20$ kcal/mol, the peptides cannot translocate. Instead, they will accumulate on the membrane surface until, in a stochastic manner, a pore forms and efflux of the entire vesicle contents occurs. Concomitant with formation of the pore, which is probably of a lipidic toroidal type, redistribution of the peptide across the membrane may also occur. Cecropin A and magainin 2 appear to belong to this group. A gray zone may exist approximately between 20 and 25 kcal/mol. Very different sequences may give rise to similar mechanisms as long as the thermodynamics of membrane binding and insertion are similar.

2 Salt bridge formation is predicted to modulate the ability of peptides to bind and translocate across the bilayer. The simplest type are intramolecular salt bridges between basic and acidic residues of the peptide. However, intermolecular salt bridges are also possible. Cell-penetrating peptides, most of which are highly cationic, such as nonaarginine or the TAT peptide, bind tightly to anionic lipids. It has been proposed that formation of peptide−lipid salt bridges allows the peptide to translocate across the bilayer (*48*, *104*−*106*).

3 The idea that peptide specificity is determined by binding is not new and is generally well accepted (*9*). However, a nuance is worth noting. For a peptide to be antimicrobial, it must bind to bacterial cells but not to eukaryotic membranes. The most obvious way of achieving this selectivity is by imparting the peptide with a positive charge, which enhances binding to anionic bacterial membranes; however, simultaneously, the level of binding to POPC bilayers or eukaryotic membranes is reduced, because of the low affinity of charged residues for a zwitterionic membrane interface (*62*). This is why antimicrobial peptides such as magainin 2 and cecropin A bind very weakly to POPC membranes (Table 2). Finally, other less investigated physical characteristics of membranes, such as headgroup size, hydrogen bonding capacity, and bilayer elastic properties, may determine the thermodynamics and specificity of peptide−membrane interactions (*57*).

4 Folding into an amphipathic α-helix concomitant with binding is essential for the types of interactions discussed. Helix formation at the interface stabilizes the membrane-bound state by ~0.4 kcal/mol per residue (*64*). Thus, for example, binding of an unfolded, 25-residue peptide to the membrane interface is weaker by 7 kcal/mol than binding of a peptide with the same amino acid composition that becomes 70% helical on the membrane surface.

Whether the formulated hypothesis and predictions prove to be correct remains to be determined. Work in our laboratories is currently in progress to test these ideas.

ACKNOWLEDGMENT

We thank Laura Huskins for performing the CD measurements.

REFERENCES

1. Hultmark, D., Steiner, H., Rasmuson, T., and Boman, H. G. (1980) Insect immunity. Purification and properties of three inducible bactericidal proteins from hemolymph of immunized pupae of *Hyalophora cecropia*. *Eur. J. Biochem. 106*, 7–16.
2. Zasloff, M. (1987) Magainins, a class of antimicrobial peptides from *Xenopus* skin: Isolation, characterization of two active forms, and partial cDNA sequence of a precursor. *Proc. Natl. Acad. Sci. U.S.A. 84*, 5449–5453.
3. Kreger, A. S., Kim, K.-S., Zaboretzky, F., and Bernheimer, A. W. (1971) Purification and properties of staphylococcal delta hemolysin. *Infect. Immun. 3*, 449–465.
4. Derossi, D., Calvet, S., Trembleau, A., Brunissen, A., Chassaing, G., and Prochiantz, A. (1996) Cell internalization of the third helix of the Antennapedia homeodomain is receptor-independent. *J. Biol. Chem. 271*, 18188–18193.
5. Green, M., and Weston, P. M. (1988) Autonomous functional domains of chemically synthesized human immunodeficiency virus tat trans-activator protein. *Cell 55*, 1179–1188.
6. Frankel, A. D., and Pabo, C. O. (1988) Cellular uptake of the tat protein from human immunodeficiency virus. *Cell 55*, 1189–1193.
7. Soomets, U., Lindgren, M., Gallet, X., Hallbrink, M., Elmquist, A., Balaspiri, L., Zorko, M., Pooga, M., Brasseur, R., and Langel, U. (2000) Deletion analogues of transportan. *Biochim. Biophys. Acta 1467*, 165–176.
8. Hällbrink, M., Floren, A., Elmquist, A., Pooga, M., Bartfai, T., and Langel, U. (2001) Cargo delivery kinetics of cell-penetrating peptides. *Biochim. Biophys. Acta 1515*, 101–109.
9. Zasloff, M. (2002) Antimicrobial peptides of multicellular organisms. *Nature 415*, 389–395.
10. Pokorny, A., and Almeida, P. F. F. (2005) Permeabilization of raft-containing lipid vesicles by δ-lysin: A mechanism for cell sensitivity to cytotoxic peptides. *Biochemistry 44*, 9538–9544.
11. Pokorny, A., Yandek, L. E., Elegbede, A. I., Hinderliter, A., and Almeida, P. F. F. (2006) Temperature and composition dependence of the interaction of δ-lysin with ternary mixtures of sphingomyelin/cholesterol/POPC. *Biophys. J. 91*, 2184–2197.
12. Wade, D., Boman, A., Wahlin, B., Drain, C. M., Andreu, D., Boman, H. G., and Merrifield, R. B. (1990) All-D amino acid-containing channel-forming antibiotic peptides. *Proc. Natl. Acad. Sci. U.S.A. 87*, 4761–4765.

13. Bessalle, R., Kapitkovsky, A., Gorea, A., Shalit, I., and Fridkin, M. (1990) All-D-magainin: Chirality, antimicrobial activity and proteolytic resistance. *FEBS Lett. 274*, 151–155.
14. Thiaudière, E., Siffert, O., Talbot, J. C., Bolard, J., Alouf, J. E., and Dufourcq, J. (1991) The amphiphilic α-helix concept. Consequences on the structure of staphylococcal δ-toxin in solution and bound to lipids. *Eur. J. Biochem. 195*, 203–213.
15. Ehrenstein, G., and Lehar, H. (1977) Electrically gated ionic channels in lipid bilayers. *Q. Rev. Biophys. 10*, 1–34.
16. Ludtke, S. J., He, K., Heller, W. T., Harroun, T. A., Yang, L., and Huang, H. W. (1996) Membrane pores induced by magainin. *Biochemistry 35*, 13723–13728.
17. Matsuzaki, K., Murase, O., Fujii, N., and Miyajima, K. (1996) An antimicrobial peptide, magainin 2, induced rapid flip-flop of phospholipids coupled with pore formation and peptide translocation. *Biochemistry 35*, 11361–11368.
18. Pokorny, A., Birkbeck, T. H., and Almeida, P. F. F. (2002) Mechanism and kinetics of δ-lysin interaction with phospholipid vesicles. *Biochemistry 41*, 11044–11056.
19. Pokorny, A., and Almeida, P. F. F. (2004) Kinetics of dye efflux and lipid flip-flop induced by δ-lysin in phosphatidylcholine vesicles and the mechanism of graded release by amphipathic, α-helical peptides. *Biochemistry 43*, 8846–8857.
20. Yandek, L. E., Pokorny, A., Floren, A., Knoelke, K., Langel, U., and Almeida, P. F. F. (2007) Mechanism of the cell-penetrating peptide Tp10 permeation of lipid bilayers. *Biophys. J. 92*, 2434–2444.
21. Shai, Y. (2002) Mode of action of membrane active antimicrobial peptides. *Biopolymers 66*, 236–248.
22. Papo, N., and Shai, Y. (2003) Can we predict biological activity of antimicrobial peptides from their interactions with model phospholipid membranes? *Peptides 24*, 1693–1703.
23. Chen, F.-Y., Lee, M.-T., and Huang, H. W. (2003) Evidence for membrane thinning effect as the mechanism for peptide-induced pore formation. *Biophys. J. 84*, 3751–3758.
24. Lee, M.-T., Hung, W.-C., Chen, F.-Y., and Huang, H. W. (2008) Mechanism and kinetics of pore formation in membranes by water-soluble amphipathic peptides. *Proc. Natl. Acad. Sci. U.S.A. 105*, 5087–5092.
25. Quian, S., Wang, W., Yang, L., and Huang, H. W. (2008) Structure of transmembrane pore induced by Bax-derived peptide: Evidence for lipidic pores. *Proc. Natl. Acad. Sci. U.S.A. 105*, 17379–17383.
26. Yang, L., Harroun, T. A., Weiss, T. M., Ding, L., and Huang, H. W. (2001) Barrel-stave model or toroidal model? A case study on melittin pores. *Biophys. J. 81*, 1475–1485.
27. Marsh, D. (2009) Orientation and peptide−lipid interactions of alamethicin incorporated in phospholipid membranes: Polarized infrared and spin-label EPR spectroscopy. *Biochemistry 48*, 729–737.
28. Langham, A. A., Sayyed Ahmad, A., and Kaznessis, Y. N. (2008) On the nature of antimicrobial activity: A model for protegrin-1 pores. *J. Am. Chem. Soc. 130*, 4338–4346.
29. Bolintineanu, D. S., Sayyed-Ahmad, A., Davis, H. T., and Kaznessis, Y. N. (2009) Poisson-Nernst-Planck models of nonequilibrium ion electrodiffusion through a protegrin transmembrane pore. *PLoS Comput. Biol. 5*, No. e1000277.
30. Grigoriev, I. V., Makhnovskii, Y. A., Berezhkovskii, A. M., and Zitserman, V. Y. (2002) Kinetics of escape through a small hole. *J. Chem. Phys. 116*, 9574–9577.
31. Berezhkovskii, A. M., and Barzykin, A. V. (2003) Escape and reentry of a Brownina particle through a hole in a cavity. *J. Chem. Phys. 118*, 6700–6701.
32. Wimley, W. C., Selsted, M. E., and White, S. H. (1994) Interactions between human defensins and lipid bilayers: Evidence for formation of multimeric pores. *Protein Sci. 3*, 1362–1373.
33. Tamba, Y., and Yamazaki, M. (2005) Single giant unilamellar vesicle method reveals effect of antimicrobial peptide magainin 2 on membrane permeability. *Biochemistry 44*, 15823–15833.
34. Rathinakumar, R., and Wimley, W. C. (2008) Biomolecular engineering by combinatorial design and high-throughput screening: Small, soluble peptides that permeabilize membranes. *J. Am. Chem. Soc. 130*, 9849–9858.
35. Gregory, S. M., Cavenaugh, A. C., Journigan, V., Pokorny, A., and Almeida, P. F. F. (2008) A quantitative model for the all-or-none permeabilization of phospholipid vesicles by the antimicrobial peptide cecropin A. *Biophys. J. 94*, 1667–1680.
36. Gregory, S. M., Pokorny, A., and Almeida, P. F. F. (2009) Magainin 2 revisited: A test of the quantitative model for the all-or-none permeabilization of phospholipid vesicles. *Biophys. J. 96*, 116–131.
37. Yandek, L. E., Pokorny, A., and Almeida, P. F. F. (2009) Wasp mastoparans follow the same mechanism as the cell-penetrating peptide transportan 10. *Biochemistry 48*, 7342–7351.
38. Yandek, L. E., Pokorny, A., and Almeida, P. F. F. (2008) Small changes in the primary structure of transportan 10 alter the thermodynamics and kinetics of its interaction with phospholipid vesicles. *Biochemistry 47*, 3051–3060.
39. Klocek, G., Schulthess, T., Shai, Y., and Seelig, J. (2009) Thermidynamics of melittin binding to lipid bilayers. Aggregation and pore formation. *Biochemistry 48*, 2586–2596.
40. Rex, S., and Schwarz, G. (1998) Quantitative studies on the melittin-induced leakage mechanism of lipid vesicles. *Biochemistry 37*, 2336–2345.
41. Brochard-Wyart, F., de Gennes, P. G., and Sandre, O. (2000) Transient pores in stretched vesicles: Role of leak-out. *Phys. A 278*, 32–51.
42. Karatekin, E., Sandre, O., Guitouni, H., Borghi, N., Puech, P. H., and Brochard-Wyart, F. (2003) Cascades of transient pores in giant vesicles: Line tension and transport. *Biophys. J. 84*, 1734–1749.
43. Evans, E., Heinrich, V., Ludwig, F., and Rawicz, W. (2003) Dynamic tension spectroscopy and strength of biomembranes. *Biophys. J. 85*, 2342–2350.
44. Huang, H. W., Chen, F.-Y., and Lee, M.-T. (2004) Molecular mechanism of peptide-induced pores in membranes. *Phys. Rev. Lett. 92*, 198304.
45. Axelsen, P. H. (2008) A chaotic pore model of polypeptide antibiotic action. *Biophys. J. 94*, 1549–1550.
46. Leontiadou, H., Mark, A. E., and Marrink, S. J. (2006) Antimicrobial peptides in action. *J. Am. Chem. Soc. 128*, 12156–12161.
47. Sengupta, D., Leontiadou, H., Mark, A. E., and Marrink, S.-J. (2008) Toroidal pores formed by antimicrobial peptides show significant disorder. *Biochim. Biophys. Acta 1778*, 2308–2317.
48. Herce, H. D., and Garcia, A. E. (2007) Molecular dynamics simulations suggest a mechanism for translocation of the HIV-1 TAT peptide across lipid membranes. *Proc. Natl. Acad. Sci. U.S.A. 104*, 20805–20810.
49. Tamba, Y., and Yamazaki, M. (2009) Magainin 2-induced pore formation in the lipid membranes depends on its concentration in the membrane interface. *J. Phys. Chem. B 113*, 4846–4852.
50. Matsuzaki, K., Murase, O., Fujii, N., and Miyajima, K. (1995) Translocation of a channel-forming antimicrobial peptide, magainin 2, across lipid bilayers by forming a pore. *Biochemistry 34*, 6521–6526.
51. Schwarz, G., and Robert, C. H. (1992) Kinetics of pore-mediated release of marker molecules from liposomes or cells. *Biophys. Chem. 42*, 291–296.
52. Ladokhin, A. S., Wimley, W. C., and White, S. H. (1995) Leakage of membrane vesicle contents: Determination of mechanism using fluorescence requenching. *Biophys. J. 69*, 1964–1971.
53. Ladokhin, A. S., Wimley, W. C., Hristova, K., and White, S. H. (1997) Mechanism of leakage of contents of membrane vesicles determined by fluorescence requenching. *Methods Enzymol. 278*, 474–486.
54. Schwarz, G., and Arbuzova, A. (1995) Pore kinetics reflected in the dequenching of a lipid vesicle entrapped fluorescent dye. *Biochim. Biophys. Acta 1239*, 51–57.
55. Arbuzova, A., and Schwarz, G. (1996) Pore kinetics of mastoparan peptides in large unilamellar lipid vesicles. *Prog. Colloid Polym. Sci. 100*, 345–350.
56. Matsuzaki, K., Yoneyama, S., and Miyajima, K. (1997) Pore formation and translocation of melittin. *Biophys. J. 73*, 831–838.
57. Pokorny, A., Kilelee, E. M., Wu, D., and Almeida, P. F. F. (2008) The activity of the amphipathic peptide δ-lysin correlates with phospholipid acyl chain structure and bilayer elastic properties. *Biophys. J. 95*, 4748–4755.
58. White, S. H., and Wimley, W. C. (1999) Membrane protein folding and stability: Physical principles. *Annu. Rev. Biophys. Biomol. Struct. 28*, 319–365.
59. Ben-Naim, A. (1978) Standard thermodynamics of transfer. Uses and misuses. *J. Chem. Phys. 82*, 792–803.
60. Holtzer, A. (1995) The "cratic correction" and related fallacies. *Biopolymers 35*, 595–602.
61. Chan, H. S., and Dill, K. A. (1997) Solvation: How to obtain microscopic energies from partitioning and solvation experiments. *Annu. Rev. Biophys. Biomol. Struct. 26*, 425–459.
62. Wimley, W. C., and White, S. H. (1996) Experimentally determined hydrophobicity scale of proteins at membrane interfaces. *Nat. Struct. Biol. 3*, 842–848.
63. Hristova, K., and White, S. H. (2005) An experiment-based algorithm for predicting the partitioning of unfolded peptides into

phosphatidylcholine bilayer interfaces. *Biochemistry 44*, 12614–12619.
64. Ladokhin, A. S., and White, S. H. (1999) Folding if amphipathic α-helices on membranes: Energetics of helix formation by melittin. *J. Mol. Biol. 285*, 1363–1369.
65. Jaysinghe, S., Hristova, K., Wimley, W., Snider, C., and White, S. H. (2009) http://blanco.biomol.uci.edu/MPEx.
66. Lee, K. H., Fitton, J. E., and Wuthrich, K. (1987) Nuclear magnetic resonance investigation of the conformation of δ-haemolysin bound to dodecylphosphocholine micelles. *Biochim. Biophys. Acta 911*, 144–153.
67. Alouf, J. E., Dufourcq, J., Siffert, O., Thiaudiere, E., and Geoffroy, C. (1989) Interaction of staphylococcal δ-toxin and synthetic analogues with erythrocytes and phospholipid vesicles. Biological and physical properties of the amphipathic peptides. *Eur. J. Biochem. 183*, 381–390.
68. Todokoro, Y., Yumen, I., Fukushima, K., Kang, S.-W., Park, J.-S., Kohno, T., Wakamatsu, K., Akutsu, H., and Fujiwara, T. (2006) Structure of tightly membrane-bound mastoparan-X, a G-protein-activating peptide, determined by solid-state NMR. *Biophys. J. 91*, 1368–1379.
69. Higashijima, T., Wakamatsu, K., Takemitsu, M., Fujino, M., Nakajima, T., and Miyazawa, T. (1983) Conformational change of mastoparan from wasp venom on binding with phospholipid membrane. *FEBS Lett. 152*, 227–230.
70. Vold, R. R., Prosser, R. S., and Deese, A. J. (1997) Isotropic solutions of phospholipid bicelles: A new membrane mimetic for high-resolution NMR studies of polypeptides. *J. Biomol. NMR 9*, 329–335.
71. Hori, Y., Demura, M., Iwadate, M., Ulrich, A. S., Niidome, T., Aoyagi, H., and Asakura, T. (2001) Interaction of mastoparan with membranes studied by ^{1}H-NMR spectroscopy in detergent micelles and by solid-state ^{2}H-NMR and ^{15}N-NMR spectroscopy in oriented lipid bilayers. *Eur. J. Biochem. 268*, 302–309.
72. Magzoub, M., Kilk, K., Eriksson, L. E. G., Langel, U., and Gräslund, A. (2001) Interaction and struture induction of cell-penetrating peptides in the presence of phospholipid vesicles. *Biochim. Biophys. Acta 1512*, 77–89.
73. Gesell, J., Zasloff, M., and Opella, S. J. (1997) Two-dimensional ^{1}H-NMR experiments show that the 23-residue magainin antibiotic peptide is an α-helix in dodecylphosphocholine micelles, sodium dodecylsulfate micelles, and trifluoroethanol/water solution. *J. Biomol. NMR 9*, 127–135.
74. Marion, D., Zasloff, M., and Bax, A. (1988) A two-dimensional NMR study of the antimicrobial peptide magainin 2. *FEBS Lett. 227*, 21–26.
75. Bechinger, B., Zasloff, M., and Opella, S. J. (1993) Structure and orientation of the antibiotic peptide magainin in membranes by solid-state nuclear magnetic resonance spectroscopy. *Protein Sci. 2*, 2077–2084.
76. Wieprecht, T., Dathe, M., Schumann, M., Krause, E., Beyermann, M., and Bienert, M. (1996) Conformational and functional study of magainin 2 in model membrane environments using the new approach of systematic double D-amino acid replacement. *Biochemistry 35*, 10844–10853.
77. Wieprecht, T., Dathe, M., Beyermann, M., Krause, E., Maloy, W. L., MacDonald, D. L., and Bienert, M. (1997) Peptide hydrophobicity controls activity and selectivity of magainin 2 amide in interaction with membranes. *Biochemistry 36*, 6124–6132.
78. Williams, R. W., Starman, R., Taylor, K. M. P., Gable, K., Beeler, T. J., Zasloff, M., and Covell, D. (1990) Raman spectroscopy of synthetic antimicrobial frog peptides magainin 2a and PGLa. *Biochemistry 29*, 4490–4496.
79. Matsuzaki, K., Nakamura, A., Murase, O., Sugishita, K., Fujii, N., and Miyajima, K. (1997) Modulation of magainin 2-lipid bilayer interactions by peptide charge. *Biochemistry 36*, 2104–2111.
80. Schumann, M., Dathe, M., Wieprecht, T., Beyermann, M., and Bienert, M. (1997) The tendency of magainin to associate upon binding to phospholipid bilayers. *Biochemistry 36*, 4345–4351.
81. Holak, T. A., Engstrom, A., Kraulis, P. J., Lindeverg, G., Bennich, H., Jones, A., Gronenborn, A. M., and Clore, G. M. (1988) The solution conformation of the antibacterial peptide cecropin A: A nuclear magnetic resonance and dynamical simulated annealing study. *Biochemistry 27*, 7620–7629.
82. Steiner, H. (1982) Secondary structure of the cecropins: Antibacterial peptides from the moth *Hyalophora cecropia*. *FEBS Lett. 137*, 283–287.
83. Marassi, F. M., Opella, S. J., Juvvadi, P., and Merrifield, R. B. (1999) Orientation of cecropin A helices in phospholipid bilayers determined by solid-state NMR spectroscopy. *Biophys. J. 77*, 3152–3155.
84. Beschiaschvili, G., and Seelig, J. (1990) Melittin binding to mixed phosphatidylglycerol/phosphatidylcholine membranes. *Biochemistry 29*, 52–58.
85. Kuchinka, E., and Seelig, J. (1989) Interaction of melittin with phosphatidylcholine membranes. Binding isotherm and lipid headgroup conformation. *Biochemistry 28*, 4216–4221.
86. Allende, D., Simon, S. A., and McIntosh, T. J. (2005) Melittin-induced bilayer leakage depends on lipid material properties: Evidence for toroidal pores. *Biophys. J. 88*, 1828–1837.
87. White, S. H., Wimley, W. C., Ladokhin, A. S., and Hristova, K. (1998) Protein folding in membranes: Determining energetics of peptide-bilayer interactions. *Methods Enzymol. 295*, 62–87.
88. Marqusee, S., and Baldwin, R. L. (1987) Helix stabilization by $Glu^{-}Lys^{+}$ salt bridges in short peptides of *de novo* design. *Proc. Natl. Acad. Sci. U.S.A. 84*, 8898–8902.
89. Wimley, W. C., Gawrisch, K., Creamer, T. P., and White, S. H. (1996) Direct measurement of salt-bridge solvation energies using a peptide model system: Implications for protein stability. *Proc. Natl. Acad. Sci. U.S.A. 93*, 2985–2990.
90. Wieprecht, T., Apostolov, O., Beyermann, M., and Seelig, J. (1999) Thermodynamics of the α-helix-coil transition of amphipathic peptides in a membrane environment: Implications for the peptide-membrane binding equilibrium. *J. Mol. Biol. 294*, 785–794.
91. Wieprecht, T., Apostolov, O., Beyermann, M., and Seelig, J. (2000) Interaction of a mitochondrial presequence with lipid membranes: Role of helix formation for membrane binding and perturbation. *Biochemistry 39*, 15297–15305.
92. van Holde, K. E., Johnson, W. C., and Ho, P. S. (1998) Principles of Physical Biochemistry , Prentice Hall, Upper Saddle River, NJ.
93. Schellman, J. A. (1955) The stability of hydrogen-bonded peptide structures in aqueous solution. *C. R. Trav. Lab. Carlsberg, Ser. Chim. 29*, 230–259.
94. Schellman, J. A. (1958) The factors affecting the stability of hydrogen-bonded polypeptide structures in solution. *J. Phys. Chem. 62*, 1485–1494.
95. Brandts, J. F. (1964) The thermodynamics of protein denaturation. II. A model of reversible denaturation and interpretations regarding the stability of chymotrypsinogen. *J. Am. Chem. Soc. 86*, 4302–4314.
96. Privalov, P. (1979) Stability of proteins: Small globular proteins. *Adv. Protein Chem. 33*, 167–241.
97. Cantor, C. R., and Schimmel, P. R. (1980) Biophysical Chemistry. Part III: The behavior of biological macromolecules, pp 1041−1073, Freeman, New York.
98. Zimm, B. H., and Bragg, J. K. (1959) Theory of the phase transition between helix and random coil in polypeptide chains. *J. Chem. Phys. 31*, 526–535.
99. Lifson, S., and Roig, A. (1961) On the theory of helix−coil transition in polypeptides. *J. Chem. Phys. 34*, 1963–1974.
100. Scholtz, J. M., Quian, H., York, E. J., Stewart, J. M., and Baldwin, R. L. (1991) Parameters of helix−coil transition theory for alanine-based peptides of varying chain lengths in water. *Biopolymers 31*, 1463–1470.
101. Marqusee, S., Robbins, V. H., and Baldwin, R. L. (1989) Unusually stable helix formation in short alanine-based peptides. *Proc. Natl. Acad. Sci. U.S.A. 86*, 5286–5290.
102. Wimley, W. C., Creamer, T. P., and White, S. H. (1996) Solvation energies of amino acid side chains and backbone in a family of hostguest pentapeptides. *Biochemistry 35*, 5109–5124.
103. Jayasinghe, S., Hristova, K., and White, S. H. (2001) Energetics, stability, and prediction of transmembrane helices. *J. Mol. Biol. 312*, 927–934.
104. Sakai, N., and Matile, S. (2003) Anion-mediated transfer of polyarginine across liquid and bilayer membranes. *J. Am. Chem. Soc. 125*, 14348–14356.
105. Sakai, N., Takeuchi, T., Futaki, S., and Matile, S. (2005) Direct observation of anion-mediated translocation of fluorescent oligoarginine carriers into and across bulk liquid and anionic bilayer membranes. *ChemBioChem 6*, 114–122.
106. Rothbard, J. B., Jessop, T. C., Lewis, R. S., Murray, B. A., and Wender, P. A. (2004) Role of membrane potential and hydrogen bonding in the mechanism of translocation of guanidinium-rich peptides into cells. *J. Am. Chem. Soc. 126*, 9506–9507.
107. Menger, F. M., Sredyuk, V. A., Kitaeva, M. V., Yaroslavov, A. A., and Melik-Nubarov, N. S. (2003) Migration of poly-L-lysine through a bilayer. *J. Am. Chem. Soc. 125*, 2846–2847.

108. Thorén, P. E. G., Persson, D., Esbjörner, E. K., Goksör, M., Lincoln, P., and Nordén, B. (2004) Membrane binding and translocation of cell-penetrating peptides. *Biochemistry 43*, 3471–3489.
109. Mitchell, D. J., Kim, D. T., Steinman, L., Fathman, C. G., and Rothbard, J. B. (2000) Polyarginine enters cells more efficiently than other polycationinc homopolymers. *J. Pept. Res. 56*, 318–325.
110. Goun, E. A., Pillow, T. H., Jones, L. R., Rothbard, J. B., and Wender, P. A. (2006) Molecular transporters: Synthesis of oligoguanidinium transporters and their application to drug delivry and real-time imaging. *ChemBioChem 7*, 1497–1515.
111. Hammond, G. S. (1955) A correlation of reaction rates. *J. Am. Chem. Soc. 77*, 334–338.